feedback scheme proposed by Preumont et al.[4] and has been shown to be L_2 stable for an arbitrary number of active struts.[3]

Kanestrøm and Egeland[5] provided an experimental investigation of impedance-adjusted active struts. A purely real impedance realization showed significantly better vibration attenuation than a parallel spring-mass-dashpot configuration, even if this could be tuned to provide better magnitude match with the structural impedance for frequencies adjacent to the resonant frequency. This dynamic impedance could however only be tuned to one resonance, and the other resonances were not affected. The real impedance, however, resulted in attenuation of all the resonances that were observed by the active strut. These results support our proposed approach.

Force Feedback Versus Bride Feedback

Now consider the bridge controller[2] given by $d(s) = -C(s)[Z'(s)f(s) - v(s)]$, where $Z'(s)$ is the mechanical impedance to be realized by the active strut and $C(s)$ is the compensator. Combining this equation with Eq. (1) gives

$$Z(s) = \frac{v(s)}{f(s)} = Z_0(s)\frac{1 + sC(s)Z'(s)/Z_0(s)}{1 + sC(s)} \tag{4}$$

If $|C(s)|$ is sufficiently large, Eq. (4) can be approximated by $Z(s) \approx Z'(s)$. The advantage of this technique is that for large $|C(s)|$ the resulting impedance is independently of the inherent impedance $Z_0(s)$ of the strut. This gives insensitivity to parameter uncertainty in $Z_0(s)$. The bridge feedback solution has the advantage of having a high in the feedback controller even if the specified impedance to be realized is small in magnitude, so that disturbances and imperfections in the actuator will be attenuated. However, it was reported by Chen and Lurie[2] that the required magnitude of $C(s)$ was not achieved, and hence there were problems in realizing $Z(s) = Z'(s)$.

In our scheme we arrive at $v(s) = [Z_0(s) + sG(s)]f(s)$. Here, $Z_0(s)$ appears in the resulting impedance $Z(s) = Z_0(s) + sG(s)$ of the strut. This it not a problem since $Z_0(s)$ is the inherent mechanical spring impedance of the open-loop strut and will hence not destabilize the system. As long as the impedance component $sG(s)$ in series with $Z_0(s)$ is strictly passive with finite gain, L_2 stability is ensured regardless of the parameter in $Z_0(s)$.[3,6] The controller $G(s)$ that realizes the impedance $Z(s) = Z_0(s) + sG(s) = Z'(s)$ is given by $G(s) = [Z'(s) - Z_0(s)]/s = Z'(s)/s - 1/K_e$. The inherent axial stiffness K_e is assumed to be large such that $K_e \gg 1$. The controller is hence dominated by the first term and may be written $G(s) \approx Z'(s)/s$ and equivalently $Z(s) \approx Z'(s)$. Hence, there will be no problems in realizing a real impedance. For the flexible structure the required impedance is so high that it in fact is unattainable and $sG(s)$ has to be tuned to the maximum value that gives stability in the presence of measurement noise and discretization and sampling effects. There will hence be a high gain in the feedback controller, and the required disturbance attenuation is obtained. A great advantage with the force feedback approach is that it requires only one requirement and avoids the use of differentiation in the control scheme.

Conclusions

Active struts are shown to provide best vibration suppression when the closed-loop strut impedance is made real and with high magnitude. In particular, the performance does not depend on knowledge of the structure's natural frequencies. The ability to suppress a specific resonance depends on where the strut is located in the structure and the limit on the controller gain. One strut absorbs power due to all the resonances that are observable at its location. The only uncertainty is the structural damping, which influences the height of the resonant peaks and hence defines the magnitude of the best controller gain. The magnitude of the structural impedance is supposed to be large at the resonant frequencies. Probably, the active strut hardware will restrict the impedance magnitude of the strut. The tuning procedure will hence be to choose the highest impedance that does not destabilize the system in the presence of measurement noise and phase lags due to a digital implementation of the controller.

A purely real, positive active strut impedance corresponds to the insertion of a dashpoint in series with the open-loop passive strut. This is realized using an integral force feedback scheme. The scheme is L_2 stable for an arbitrary number of active struts and is attractive since it avoids the use of differentiation.

Acknowledgments

This work was supported by the Norwegian Space Center and NFT A/S.

References

[1]Nilsson, J. W., *Electric Circuits*, Addison–Wesley, Reading, MA, 1983, Chap. 11.

[2]Chen, G.-S., and Laurie, B. J., "Active Member Bridge Feedback Control for Damping Augmentation," *Journal of Guidance, Control, and Dynamics*, Vol. 15, No. 5, 1992, pp. 1155–1160.

[3]Kanestrøm, R. K., and Egeland, O., "Nonlinear Active Vibration Damping," *IEEE Transactions on Automatic Control*, Vol. 39, No. 9, 1994, pp. 1925–1928.

[4]Preumont, A., Dufour, J.-P., and Malékian, C., "Active Damping by a Local Force Feedback with Piezoelectric Actuators," *Journal of Guidance, Control, and Dynamics*, Vol. 15, No. 2, 1992, pp. 390–395.

[5]Kanestrøm, R. K., and Egeland, O., "Impedance Adjusted Active Strut," *Proceedings of the 1994 American Control Conference*, Vol. 2, Baltimore, MD, 1994, pp. 1462–1466.

[6]Kanestrøm, R. K., "Active Vibration Damping of Large Flexible Space Structures," Ph.D. Dissertation, Norwegian Inst. of Technology, 1994.

Two Misconceptions in the Theory of Inertial Navigation Systems

Itzhack Y. Bar-Itzhack*
Technion—Israel Institute of Technology, Haifa 32000, Israel

I. Introduction

THE purpose of this Note is to point out prevailing wrong explanations of two basic facts in the operation of inertial navigation systems (INSs) and provide the correct explanation for them.

II. Gyrocompassing

A. Misconception

Principle of Operation

For simplicity let us consider the gyrocompassing process of a stable platform INS. Denote Earth rate by Ω and latitude by λ; then it is well known that Ω_N, the local north component of Earth rate at a point on Earth whose latitude angle is λ, is given by $\Omega_N = \Omega\cos\lambda$. Due to azimuth misalignment, the platform north and east coordinate axes, N_p and E_p, respectively (see Fig. 1), are rotated by the azimuth misalignment angle ψ_D with respect to N and E, the reference, local level local north (LLLN) coordinate system. The projection of Ω_N on the platform coordinate axes yields the component $-\Omega_N \sin\psi_D$ along the E_p axis that, for a small ψ_D, becomes $-\Omega_N\psi_D$. The east platform gyroscope, which measures rates along the E_p axis, measures the component $-\Omega_N\psi_D$, which is treated as a platform drift error and is fed into the platform control system. The latter, in an attempt to cancel the unwanted drift, torques the platform in an opposite direction and thus causes the platform to drift about its east axis by the rate $\Omega_N\psi_D$. To this drift we add

Presented as Paper 93-3819 at the AIAA Guidance, Navigation, and Control Conference, Monterey, CA, Aug. 9–11, 1993; received Oct. 4, 1993; revision received May 21, 1994; accepted for publication Sept. 14, 1994.

*Sophie and William Shamban Professor of Aeronautics, Faculty of Aerospace Engineering; Head, Flight Control Laboratory; Member, Technion Space Research Institute.

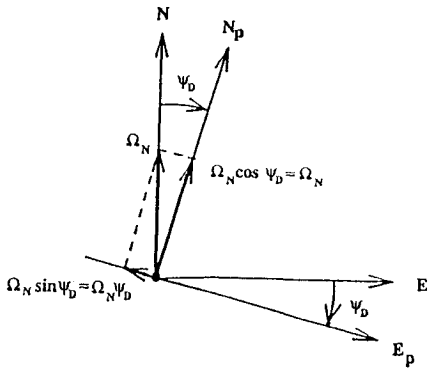

Fig. 1 Coordinate axes during gyrocompassing.

the platform drift due to the east gyroscope own drift rate ε_E. Since the platform is already level, the down component of Earth rate has no projection on the E_p axis. Consequently, the total platform drift about its east axis E_p is

$$\dot{\psi}_E = \Omega_N \psi_D + \varepsilon_E \tag{1}$$

As a result, ψ_E starts building up, which brings the north platform axis N_p up from its level position and causes the north platform accelerometer to read a projection of the gravity vector $\bar{g}$. This projected quantity of $\bar{g}$ is interpreted by the INS as an acceleration a_N along the LLLN north axis; that is, $a_N = g\psi_E$. In the process of computing the nominal north velocity component, a_N is integrated by the INS computer and yields the erroneous north velocity component v_N. In other words, $\dot{v}_N = a_N$ and therefore $\dot{v}_N = g\psi_E$. Since, as seen from Eq. (1) and the latter equation, v_N is indicative of the azimuth misalignment angle ψ_D, in old INS, v_N was fed into a control loop that torqued the platform about its down axis in order to eliminate ψ_D. Nowadays, v_N is fed into an extended Kalman filter in order to estimate ψ_D and then remove it.

Lower Limit

The gyrocompassing process has a lower limit that is a function of the east gyroscope drift rate ε_E. Indeed, gyrocompassing comes to a halt when v_N, the indicator of the existence of ψ_D, is driven down to zero. Obviously, a necessary condition for v_N to stay zero is $\dot{v}_N = 0$. This happens only if

$$0 = \Omega_N \psi_D + \varepsilon_E \tag{2}$$

which yields the lower limit on ψ_D:

$$|\psi_{D,\min}| = \frac{|\varepsilon_E|}{\Omega_N} = \frac{|\varepsilon_E|}{\Omega \cos \lambda} \tag{3}$$

This is the well-known lower limit of the gyrocompassing process.

Discussion

The preceding explanation yields the correct results obtained when the gyrocompassing process takes place. However, there are two instances where the fallacy of the preceding explanation is encountered. First, when we use it to consider the inertial rotation of the platform about its north axis N_p and, second, when a monitor gyroscope (MG) is used in order to calibrate the platform north and east gyroscopes. Let us focus our attention on the latter.

An MG is used to evaluate the drift of the gyroscope it monitors.[1] During the evaluation process, the MG is set to read the input signal of the monitored gyroscope. When measuring or evaluating the expected measurement of the MG while it is set to monitor the east platform gyroscope, one realizes that the nominal, error-free measurement, of the monitor gyroscope is zero and not $-\Omega_N \psi_D$. This, of course, contradicts the underlying assumption of the preceding explanation that the east gyroscope measures the quantity $-\Omega_N \psi_D$.

B. Correct Explanation: Principle of Operation

Indeed, as described before, for small ψ_D the projection of Ω_N on the platform coordinate axes yields the component $-\Omega_N \psi_D$ along the E_p axis. However, the platform east gyroscope, which measures rates along the E_p axis, does not measure the component $-\Omega_N \psi_D$ and the latter is not treated as a platform drift error and thus it is not fed into the platform control system. Therefore the control system does not torque the platform in an opposite direction in an attempt to cancel this component. On the contrary, the component $-\Omega_N \psi_D$ is the rate by which Earth turns about E_p and, therefore, is also the rate by which the platform has to be torqued about E_p in order to follow the rotation of Earth with respect to inertial space and thereby stay level with respect to Earth. Since the platform is not torqued by this rate, Earth is moving away from the platform in an opposite direction to $-\Omega_N \psi_D$. Therefore the N_p axis retreats from the earth surface by the rate $\Omega_N \psi_D$ about the E_p axis. Therefore although the preceding explanation resulted in the correct effect, the reason given to it was wrong.

The east gyroscope own drift rate, ε_E, does indeed force the platform to drift with respect to inertial space as well as to the Earth surface by the rate ε_E. (Note that the platform drift rate is opposite to the gyroscope drift that causes it. However, in stable platforms it is customary to denote the platform drift by the symbol assigned to the drift of the gyroscope that causes it.[2] The difference between the two is just a sign difference.) The net rate of change of ψ_E is $\Omega_N \psi_D + \varepsilon_E$, which gives rise to Eq. (1) and therefore to Eq. (3), which is indeed the well-known lower limit of the gyrocompassing process.

We realize that the latter explanation is the correct one since although explaining the well-known phenomena that take place during the gyrocompassing process, it also explains correctly the readings obtained when using an MG for monitoring the horizontal gyroscope readings.

III. Schuler Oscillations

A. Misconception

Figure 2 presents the geometry used in one of the popular, easy-to-understand explanations[3] of the generation of the famous Schuler oscillation characteristic of INS. For the sake of the explanation, it is assumed that the INS is of the stable platform kind. We assume that the INS traverses on the equator. We start the explanation by considering the effect an accelerometer bias has on the INS error propagation; therefore, we assume that the only error source in the system is δa, the bias of the accelerometer that points along the trajectory. The INS starts its traverse at point P_0. After a certain time, the INS reaches point P_t; however, due to the existence of δa, the INS computer computes the INS location to be at P_c. Since the INS computer torques the platform to be level at the computed position, the platform is tangent to Earth at point P_c. But the platform is truly at point P_t; therefore, at point P_t the platform is not level. We denote the platform mislevel angle by $\delta\theta$. Due to this mislevel, the gravity vector has a component along the accelerometer axis. The size of this component is $g \sin \delta\theta$, which for a small tilt angle can be approximated by $g\,\delta\theta$. The specific force f that the accelerometer reads is given therefore by $f = a - g\,\delta\theta$, where a is the correct acceleration along the trajectory. The accelerometer reading f_r is the sum of f and the accelerometer bias; that is, $f_r = f + \delta a$. Note

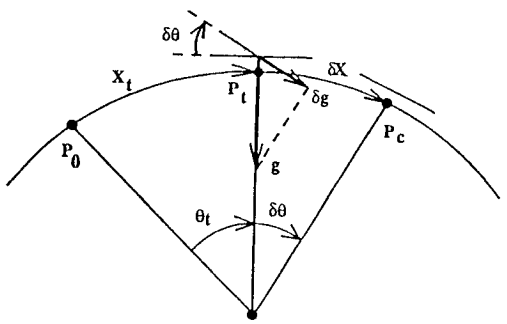

Fig. 2 Geometric illustration of elements involved in explanation of generation of Schuler oscillations on spherical Earth.

that since nominally the platform is supposed to be perpendicular to $\bar{g}$, the computer is not programmed to extract a from f. Therefore, when the traverse starts from rest at P_0 the computed arc, which we denote by X_c, traveled by the INS is given by

$$X_c = \int\int f_r \, dt \, dt = \int\int (a + \delta a - g\,\delta\theta) \, dt \, dt \tag{4}$$

We can separate X_c into the true traversed arc X_t and the INS-generated error δX; that is, we can write $X_c = X_t + \delta X$. Obviously

$$X_t = \int\int a \, dt \, dt \tag{5}$$

and thus

$$\delta X = \int\int (\delta a - g\,\delta\theta) \, dt \, dt \tag{6}$$

Differentiation of Eq. (6) twice yields $\delta\ddot{X} = \delta a - g\,\delta\theta$. It is obvious from Fig. 2 that $\delta\theta = \delta X/R$, where R is the radius of Earth; consequently

$$\delta\ddot{X} + (g/R)\delta X = \delta a \tag{7}$$

Equation (7) is the equation of a harmonic oscillator driven by δa. The frequency of the oscillation is $f = \sqrt{g/R}/2\pi$. This oscillation is known as Schuler oscillations. Its period is 84.6 min.

The previous explanation of the generation of the Schuler oscillation relies on a traverse on a spherical Earth and the fact that the platform is torqued over the sphere in order to level the platform at any point on Earth at which the platform is located. This torquing is sometimes called Schuler tuning. It is said quite often, and indeed, one gets then the impression that this torquing (Schuler tuning) is the source of the oscillation. As will be shown next, this is not true.

B. Another Explanation

In order to show that torquing of the platform to be locally level with respect to the surface of Earth is not the cause of the Schuler oscillations, we will show that Schuler oscillations exists also in INSs whose platform is not torqued to be locally level. To meet this end, we develop next the one-dimensional position error equation in tangent plane coordinates[4] that have the quality of not being torqued to be locally level with respect to the surface of Earth. Figure 3 presents the geometry governing this case. The origin of the coordinate system is at point X_0. From Fig. 3 it is seen that the specific force f that the accelerometer reads in the X direction is $f = a + g\tan\alpha$, and since $\tan\alpha = X_t/R$,

$$f = a + (g/R)X_t \tag{8}$$

The accelerometer reading contains also the accelerometer bias:

$$f_r = f + \delta a = a + (g/R)X_t + \delta a \tag{9}$$

At a certain time the INS is at point X_t; however, due to the accelerometer bias error δa, the INS computer calculates the INS position as X_c.

The computer is programmed to remove the gravitational component from f_r; however, since the computer computes X_c as X_t, it uses the former to extract the acceleration from f_r therefore form (9), the computed acceleration is

$$a_c = f_r - (g/R)X_c = a + (g/R)(X_t - X_c) + \delta_a \tag{10}$$

and since $X_c = X_t + \delta X$, we can write Eq. (10) as

$$a_c = a - (g/R)\delta X + \delta a$$

The computer performs

$$X_c = \int\int \left(a - \frac{g}{R}\delta X + \delta a\right) dt \, dt \tag{11}$$

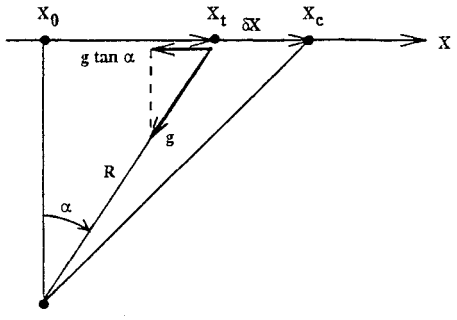

Fig. 3 Geometric illustration of elements involved in explanation of generation of Schuler oscillations in tangent plane coordinates.

whereas the true position X_t is computable as

$$X_t = \int\int a \, dt \, dt \tag{12}$$

From Eqs. (11) and (12) we obtain

$$X_c = X_t + \int\int \left(-\frac{g}{R}\delta X + \delta a\right) dt \, dt \tag{13}$$

It follows that

$$\delta X = \int\int \left(-g\frac{\delta X}{R} + \delta a\right) dt \, dt \tag{14}$$

Differentiating Eq. (14) twice yields the desired result:

$$\delta\ddot{X} + (g/R)\delta X = \delta a \tag{15}$$

We realize that Eq. (15) is identical to Eq. (7), and therefore all that was said about the existence of the Schuler oscillations in the preceding explanation holds here too.

C. Correct Reason for Schuler Oscillations

As seen from the foregoing explanation, Schuler oscillations occur also in INSs that are not torqued in order to stay locally level. Consequently, the torquing of the platform with respect to Earth is definitely not the reason for Schuler oscillations. What is then the cause of the oscillations? From the last explanation we observe that there are two factors that together bring about the Schuler oscillations. One of them is the fact that accelerometers cannot distinguish between acceleration and gravity; that is, they measure both (specific force). Therefore, to perform the navigation computation, we have to remove the gravity part of the accelerometer reading. However, gravity is calculated as a function of the computed position. Therefore the removal of gravity generates a feedback link that is a necessary condition for the generation of oscillations. We note, though, that while the removal of the gravity component from the horizontal channels in a stable platform is entrusted to the platform control mechanism, which is supposed to keep the platform level and hence keep the gravity away from the horizontal channels, in a strapdown INS, as well as in tangent plane mechanization, this is done computationally. The second factor necessary for the generation of Schuler oscillations is the gravity field being a central field; that is, all gravity vectors in a certain neighborhood point to a common point in space.

IV. Summary

In this Note we have discussed two widely spread misconceptions in INSs: one concerning gyrocompassing and the other concerning Schuler oscillations.

First we presented the wrong explanation of the gyrocompassing process and explained that the fallacy of this explanation is exposed when analyzing the operation of an MG. We then gave the correct explanation.

Next we discussed the generation of the Schuler oscillations. We presented a widespread explanation of the generation of the oscillations from which it could be concluded that the reason for the

oscillations is the torquing of the INS platform. Using tangent plane coordinates, it was then shown that the torquing was not the reason. We then explained that Schuler oscillations stem from two factors acting together. One is the fact that accelerometers measure specific force rather than acceleration and therefore the gravity part of the accelerometer reading needs to be removed, thereby creating a feedback loop. The second factor is the gravity field being a central field. Although the explanations given here utilized stable platforms, the same can be shown for strapdown INSs.

References

[1]Gelb, A., "Synthesis of a Very Accurate Inertial Navigation System," *IEEE Transactions on Aerospace and Navigation Electronics*, Vol. 12, June 1965, pp. 119–128.

[2]Weinreb, A., and Bar-Itzhack, I. Y., Authors' reply to Benson, D. O., "Comment on 'The Psi-Angle Error Equation in Strapdown Inertial Navigation Systems,' " *IEEE Transactions on Aerospace and Electronic Systems*, Vol. AES-15, No. 1, 1979, pp. 169, 170.

[3]Brown, R. G., "Notes on Inertial Navigation," Electrical Engineering Dept., Iowa State Univ., Ames, IA, June 1968 (class notes, pp. 4–8).

[4]Russell, W. T., "Theory of Inertial Navigation," *Inertial Guidance*, edited by R. G. Pitman, Wiley, New York, 1962, p. 30.

Controllability and Optimization in Aeroassisted Orbital Transfer

R. Andiarti* and C. H. Moog†
Laboratoire d'Automatique de Nantes, 44072 Nantes, France
and
J. Szymanowski‡
Warsaw University of Technology, 00-665 Warsaw, Poland

I. Introduction

THIS Note addresses the atmospheric flight phase of an aeroassisted orbital transfer maneuver of a spacecraft. The re-entry mission of such a spacecraft has been studied recently by Roenneke and Cornwell.[1] The primary objective is to relate the computation of optimal trajectories to the controllability properties of the spacecraft. The vehicle is assumed to be controlled by the bank angle and is to perform a zero orbital plane change with some fixed exit conditions. A performance index is chosen such that the exit velocity error and the exit wedge angle will be minimized.

Commonly, employed optimization procedures are based on the iterated shooting method.[2] Such procedures are known to be highly sensitive to the initialization of the adjoint vector. Finding an initial condition of the adjoint vector that ensures the convergence of the optimization procedure is often problematic. Indeed, the initial adjoint vector must be chosen close to the optimum value, which is of course not known a priori. The goal of this Note is not to contribute to optimization theory but rather to highlight the controllability aspects that render the optimization problem ill conditioned. This will enable the systematic use of optimization for generating trajectories in those areas where the optimization problem is well posed. Indeed, in the higher layers of the atmosphere, the atmospheric density is small and the spacecraft's controllability vanishes. Simulations show that the optimal-control method is more efficient when applied in the lower layers of the atmosphere.

The Note is organized as follows. In Sec. II, the equations of motion of the vehicle are described, and in Sec. III the optimal-control method is outlined. The controllability analysis is presented in Sec. IV, and finally, the simulation results are given in Sec. V.

II. Model Equations

The basic equations for orbital transfer are those for deorbit, atmospheric flight, boost, and circularization or reorbit. For guidance purpose, however, we consider only the atmospheric flight portion of the maneuver. The aerodynamic forces are limited to *drag* and *lift*, and the vehicle is assumed to be axisymmetric. The equations of motion of the center of mass are given by

$$\dot{r} = V \sin\gamma$$

$$\dot{\tau} = V \cos\gamma \cos\chi/(r\cos\delta)$$

$$\dot{\delta} = V \cos\gamma \sin\chi / r$$

$$\begin{aligned}
\dot{\chi} &= -\frac{\boldsymbol{L}\sin\sigma}{mV\cos\gamma} - \frac{V}{r}\cos\gamma\cos\chi\tan\delta - 2\omega(\sin\delta \\
&\quad - \tan\gamma\cos\delta\sin\chi) - \frac{\omega^2 r}{V\cos\gamma}\sin\delta\cos\delta\cos\chi \qquad (1)\\
\dot{V} &= \frac{\boldsymbol{D}}{m} - \frac{\mu}{r^2}\sin\gamma + \omega^2 r\cos\delta(\sin\gamma\cos\delta \\
&\quad - \cos\gamma\sin\delta\sin\chi)\\
\dot{\gamma} &= -\frac{\boldsymbol{L}\cos\sigma}{mV} + \left(\frac{V}{r} - \frac{\mu}{r^2 V}\right)\cos\gamma + 2\omega\cos\delta\cos\chi \\
&\quad + \frac{\omega^2 r}{V}\cos\delta(\cos\gamma\cos\delta + \sin\gamma\sin\delta\sin\chi)
\end{aligned}$$

where $\boldsymbol{D}$ and $\boldsymbol{L}$ are the drag and lift forces, r is the distance from the center of Earth, δ is the latitude, τ is the longitude, V is the velocity, γ is the flight path angle, χ is the heading angle, m is the vehicle's mass (=1408.6 kg), C_D and C_L are the drag and lift coefficients, σ is the bank angle, ω is the angular velocity of Earth (=0.729 10^{-4} rad/s), and μ is the gravitational constant of Earth (=0.3986 10^{15} m^3/s^2). The simulation results presented later use the 1976 U.S. Standard Atmosphere.

III. Optimal Control

The objective is to bring the spacecraft from a high orbit to a low orbit using the natural braking action of the atmosphere. Certain atmospheric exit conditions have to be fulfilled so that the vehicle reaches the low orbit with a suitable velocity. These conditions consist of a given atmospheric exit velocity and zero exit wedge angle η. In order to match the final conditions, the following performance index is minimized:

$$\mathcal{J} = g_1(\Delta h)^2 + g_2(\Delta V)^2 + g_3(\eta)^2 \qquad (2)$$

where g_1, g_2, g_3 are positive, Δh represents the final altitude error, ΔV is the atmospheric exit velocity error, and η is the final wedge angle.

By using the principle of conservation of energy and angular momentum at the atmospheric exit and the point of the low orbit, the relation between the exit velocity ($\tilde{V}_f$) and the exit flight path angle ($\tilde{\gamma}_f$) computed in an inertial system is derived. This relation is expressed by[3]

$$r_l^2\left(2V_{at} - \tilde{V}_f^2\right) - 2r_l r_a V_{at}^2 + r_a^2 \tilde{V}_f^2 \cos^2\tilde{\gamma}_f = 0 \qquad (3)$$

where r_a is the radius of atmospheric boundary, V_{at} is the circular velocity at $r = r_a$, and r_l is the radius of a low orbit to reach in the next phase of the maneuver. Equation (3) guarantees that, after

Received Jan. 25, 1994; revision received June 10, 1994; accepted for publication July 25, 1994.

*Ph.D. Student, Unité Associée au Centre National de la Recherche Scientifique, Ecole Centrale de Nantes/University of Nantes, 1 rue de la Noë.

†Chargé de Recherche, Unité Associée au Centre National de la Recherche Scientifique, Ecole Centrale de Nantes/University of Nantes, 1 rue de la Noë.

‡Professor, Institute of Automatic Control, Nowowiejska 15/17.